Mass Transport in Unsteady Shallow-Water Waves

Akira ISHIDA, Wataru KIOKA and Kouji ASADA *
Department of Architecture, Urban Engineering and Civil Engineering
(Received July 26,1985)

* Prefectural Office of Kanazawa

ABSTRACT

Progressive waves advancing into shallow water region are expected to be unsteady due to the near-resonance. The velocity field associated with such a nonlinear shallow-water wave is determined theoretically using the numerical results obtained previously, and neglecting viscosity the equation of mass-transport velocity is derived for both infinite and closed-ended channels. The results indicate that the mass transport induced by unsteady water waves is eventually unsteady and the spatial variations of the drift become increasingly significans with the increase of Ursell number. This feature may result in the circulating currents in a closed-ended channel. Experements are conducted to examine the theoretical predictions.

INTRODUCTION

The mass transport in progressive water waves, first noticed by *Stokes* (1847), is a subject of great interest to coastal investigators as it plays a role in the local circulation pattern and sediment transport. *Longuet-Higgins* (1953) for the first time derived the laminar boundary-layer conduction solution based on sinusoidal wave theory to predict the drift velocity close to the bed. His solution was later examined by *Ünlüata and Mei* (1970) using the Lagrangian description of the boundary layer. The calculation of mass transport based on the shallow-water wave approximation was carried out in the recent studies ; a second approximation with Stokes wave theory by *Sleath* (1972) and that with Cnoidal wave theory by *Isaacson* (1976).

Assumptions commonly made in the work cited are that waves are steady and propagating on a rigid and smooth bed. From sand bed model tests for waves of the shallow water range, it has become clear that the values of the mass-transport velocity vary spatially, and as a result the circulation of the current takes place along the wave channel (see *Ishida et al.*, 1983). This tendency is considerably different from the results predicted by afore-mentioned theories. The experimental results suggest that the mass transport can be affected by the presence of secondary waves. It should be noted that progressive waves in the shallow water are inevitably unsteady due to the near-resonance as described by *Phillips* (1960) and thus the secondary waves observed in the laboratory are present in the nature. The study of the effect of such unsteady waves is of great importance for better understanding of the mass transport in the shallow water.

The aim of this study is to develop an expression for the mass-transport velocity which takes account of the presence of secondary waves and to investigate the mass transport under unsteady shallow-water waves on the sand bed. The influence of viscosity is neglected assuming that the viscosity would cause the secondary effect on the mass transport for the case of movable bed. Although the interaction between the fluid and bed is sufficiently complex that it is not satisfactorily predicted by existing theorise, it may be remarked that the sand moves in the direction of oscillatory flow, in other words the non-slip condition is not satisfied on the boundary of movable bed. Experiments are also carried out to test theoretical predictions obtained, specifically for shallow-water waves progressing over the sand bed in the closed-ended wave channel.

THEORETICAL INVESTIGATIONS

Consider a deep-water wave of sinusoidal shape advancing into a shallow-water region. In the shallow water the dispersion relation between frequency and wave number can be regarded as nearly linear. Under this condition, according to *Phillips* (1960) the second-order near-resonance takes place and some of the energy of sinusoidal wave is transfered to the second-order free wave. In this connection *Mei* (1983) applied a naive perturbation method to the KdV equation and found that the amplitude of the second-order free wave is resonated to grow linearly with the distance traveled until it becomes comparable with the amplitude of the fundamental component. The Ursell number has shown to prescribe the significance of the nonlinear interaction. As for the case of harmonic motion of the wave maker, *Fontanet* (1961) showed by solving the Lagrangian equations of fluid motion that a second-order free wave is generated when the relative water depth to wavelength is small.

The generation of second-order and possibly higher order free waves renders the progressive waves unsteady. Accordingly the surface elevation of the shallow-water wave should be expressed in the general form

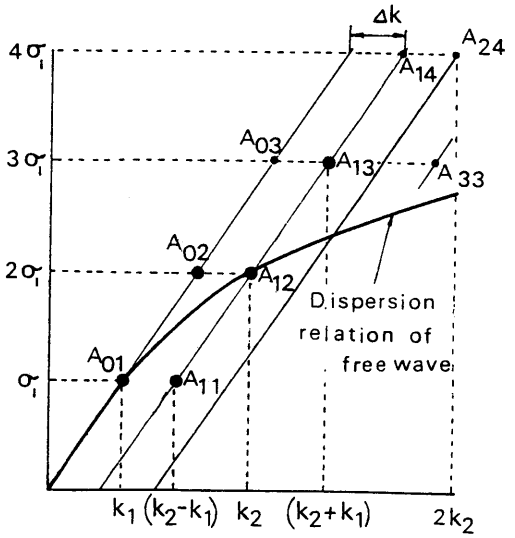

Fig. 1 : Interpretation of the spectral components in wave-number and freqency.

$$\eta(x,\ t)=\sum_{n=0}^{N}\sum_{m=1}^{M}A_{nm}\cos(k_{nm}x-\sigma_m t+\theta_{nm}) \qquad (1)$$

where A_{nm} is the amplitude of the spectral component in wave-number k_{nm} and frequency σ_m, and θ_{nm} is the initial phase. In this equation N and M denote the total number of the spectral components used to describe the unsteady wave profile and vary depending on the Ursell number. The wave-number k_{nm} and frequency σ_m are composed of elements, with each element being the sum or difference of other components. The amplitude A_{nm} may be obtained from the double Fourier series expansion analysis of $\eta(x, t)$.

Fig. 1 shows the two-dimensional wave components in relation to wave-number and frequency. Henceforth, as indicated in this figure, the notation A_{nm} for the wave amplitude will be also used to denote the correspoding wave component itself for convenience. Thus the fundamental component A_{01} and the second-order free wave A_{12} correspond to (k_1, σ_1) and $(2k_1+\Delta k=k_2, 2\sigma_1)$, respectively. The sum-wave and difference-wave components, A_{13} and A_{11}, are induced by the nonlinear interaction between A_{01} and A_{12}. A set of components lying along the line through the origin, A_{01}, A_{02}, A_{03} and so forth, constitutes the nonlinear waves of permanent type such as Stokes waves. The other components contribute to the deformation.

Extensive numerical studies of the KdV equation for the initially given sinusoidal waves with various wave heights H, water depths h and wave periods T have been carried out by *Ishida et al.* (1979, 1980 and 1981) using the method of *Zabusky and Kruskal* (1965). They have shown that the resultant wave amplitude A_{nm} can be expressed as a function of the Ursell number Ur. Eq. (1) is then rewritten as

$$\eta(x,\ t)=\frac{H}{2}\sum_{n=0}^{N}\sum_{m=1}^{M}\xi_{nm}\cos\{(mk_1+n\Delta k)x-m\sigma_1 t+\theta_{nm}\} \qquad (2)$$

$$\xi_{nm}=\alpha(\log U_r)^2+\beta\log U_r+\gamma \qquad (3)$$

where $Ur=HL^2/h^3$, $k_1=2\pi/L$ and $\sigma_1=2\pi/T$, with L being the wavelength corresponding to the primary free wave of period T. The mismatch of wave-number Δk introduced in Eq. (2) has rele-

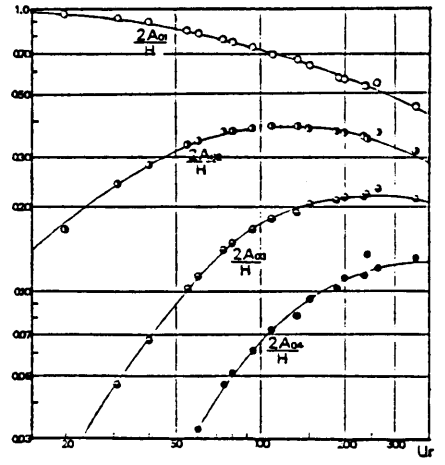

(a)

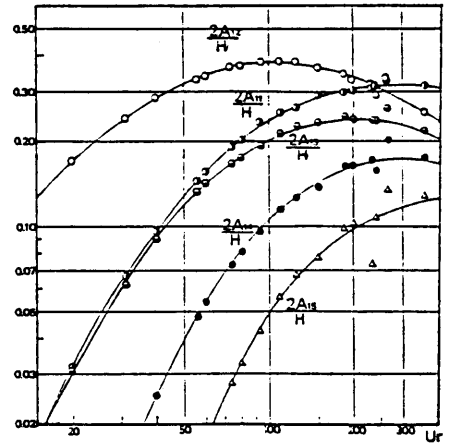

(b)

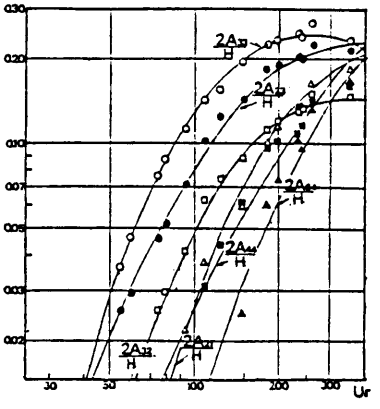

(c)

Fig. 2 : Normalized amplitudes $\xi_{nm}=2A_{nm}/H$ are plotted as a function of the Ursell number Ur (*Ishida et al.*, 1980)

Table 1 : Coefficients α, β, and γ, and phase angles θ_{nm} involved in Eqs. (2)−(3).

ξ_{nm}	α	β	γ	θ_{nm}
ξ_{01}	-0.137	0.263	-0.118	0
ξ_{02}	-0.536	2.273	-2.817	0
ξ_{03}	-0.876	4.143	-5.552	0
ξ_{04}	-1.182	5.901	-8.258	0
ξ_{11}	-0.865	4.108	-5.379	π
ξ_{12}	-0.646	2.607	-3.075	π
ξ_{13}	-0.903	4.163	-5.406	π
ξ_{14}	-1.202	5.876	-7.929	π
ξ_{15}	-1.300	6.726	-9.601	π
ξ_{21}	-1.807	9.881	-14.136	0
ξ_{23}	-1.450	7.396	-10.071	π
ξ_{32}	-2.079	10.351	-13.714	π
ξ_{33}	-2.111	10.045	-12.543	0
ξ_{44}	-0.159	2.528	-6.045	0

vance to the overtake length Lov, the distance between two stations where the secondary crests have equal strength, as follows:

$$\Delta k = k_2 - 2k_{11} = 2\pi/L_{ov} \tag{4}$$

The amplitude ratio of the spectral component to the initial wave ξ_{nm} is shown in Fig. 2 as a function of Ur. Note that the ratio ξ_{24} is extremely small and therefore is not shown here. For the values of Ur less than about 50, the ratios ξ_{01}, ξ_{02}, ξ_{11}, ξ_{12} and ξ_{13} are given larger than 0.1. with the increase in Ur, however, in addition to these five components the other components ξ_{03}, ξ_{14} and ξ_{33} become increasingly significant. The coefficients α, β and γ determined from Fig. 2 as well as the phase angles θ_{nm} are presented in Tabel 1. In determining θ_{nm}, θ_{01} is chosen to be zero. The normalized celerities have been obtained for both primary and secondary waves in the work of Ishida et al. (1981) (see Fig. 3). From their results the dispersion relation of primary (m=1) and second-order (m=2) free waves may be expressed in the form

$$\log\left(\frac{C_m}{\sqrt{gh}}\right)=\alpha'\{\log(T\sqrt{g/h})\}^2+\beta'(T\sqrt{g/h})+\gamma' \tag{5}$$

where the coefficients α', β' and γ' for $m=1$ are given with the parameter of H/h as

$$\left.\begin{aligned}\alpha' &= 0.387(H/h)^2-0.537(H/h)-0.012\\ \beta' &= -1.094(H/h)^2+1.567(H/h)+0.075\\ \gamma' &= 0.797(H/h)^2-1.014(H/h)-0.093\end{aligned}\right\} \tag{6}$$

and for $m=2$

$$\alpha' = -2.803(H/h)^2+1.635(H/h)-0.057$$

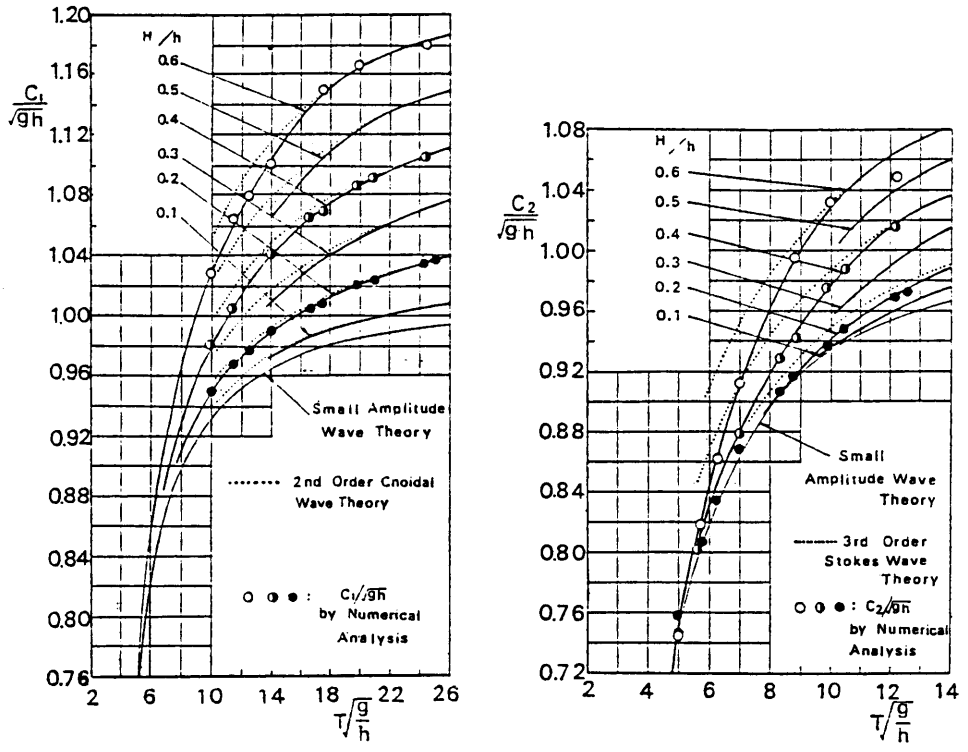

Fig. 3 : Normalized celerities of the primary and second-order free waves are plotted as a function of $T\sqrt{g/h}$ (*Ishida et al.*, 1981)

$$\left.\begin{aligned}\beta' &= 5.270(H/h)^2-2.834(H/h)+1.256\\ \gamma' &= -2.372(H/h)^2+1.223(H/h)-0.721\end{aligned}\right\} \quad (7)$$

As can be seen from Fig. 3, Eq. (5) assumes close agreement with the cnoidal wave theory for larger values of $T\sqrt{g/h}$ and the Stokes wave theory for smaller values of $T\sqrt{g/h}$. At very small $T\sqrt{g/h}$ the computed celerities approach the curve obtained from the linear wave theory.

To estimate the mass ransport, we next seek the potential function that can represent the inner velocity field associated with the wave deformation described in the foregoing analysis. Exact expressions of the velocity potential, however, are not straightforwardly attainable in the present case because the analysis involves all high order nonlinear components. To this end, we restrict our attention to the cases of relatively small Ursell number so that the second-order interactions between two free waves would play a central role in the wave deformation. The problem considered here, that is, the second-order interactions of two primary waves in the water of finite depth, has been treated and solved using the perturbation procedure in powers of wave steepness by *Hamada* (1965). We omit the details of the process and merely reproduce the solutions here. Namely, the second order approximation to the velocity potential is

$$\begin{aligned}\phi = {} & a_1\sigma_1\frac{\cosh k_1(h+z)}{\sinh k_1 h}\sin S_1 + 2a_2\sigma_1\frac{\cosh k_2(h+z)}{\sinh k_2 h}\sin S_2\\ & + B_{21}\frac{\cosh 2k_1(h+z)}{\sinh 2k_1 h}\sin 2S_1 + B_{22}\frac{\cosh 2k_2(h+z)}{\sinh 2k_2 h}\sin 2S_2\\ & + B_{23}\frac{\cosh(k_1+k_2)(h+z)}{\sinh(k_1+k_2)h}\sin(S_1+S_2) + B_{24}\frac{\cosh(k_1-k_2)(h+z)}{\sinh(k_1-k_2)h}\sin(S_1-S_2)\end{aligned} \quad (8)$$

with the notations of

$$\left.\begin{aligned} S_1 &= k_1 x - \sigma_1 t + \theta_1 \\ S_2 &= k_2 x - 2\sigma_1 t + \theta_2 \end{aligned}\right\} \quad (9)$$

where a_1, σ_1 and k_1 are the amplitude, frequency and wave-number of the primary wave respectively, and a_2, $2\sigma_1$ and k_2 are those of another free wave. The coefficients B_{21}, B_{22}, B_{23} and B_{24} are uniquely determined from the values of a_1, a_2, σ_1, k_1, k_2 and h (see *Hamada,* 1965). It may be noted that in this case the dispersion relation for primary and secondary free waves is identical to that of linear wave theory. The corresponding wave profile is given by

$$\left.\begin{aligned} \eta(x,\ t) &= a_1 \cos S_1 + a_2 \cos S_2 \\ &+ \frac{1}{g}\left\{2\sigma_1 B_{21} coth\ 2k_1 h - \frac{1}{4} a_1^2 \sigma_1^2 (coth^2 k_1 h - 3)\right\} \cos 2S_1 \\ &+ \frac{1}{g}\left\{4\sigma_1 B_{22} coth\ 2k_2 h - a_2^2 \sigma_1^2 (coth^2 k_2 h - 3)\right\} \cos 2S_2 \\ &+ \frac{1}{g}\left\{3\sigma_1 B_{23} coth(k_1 + k_2) h - a_1 a_2 \sigma_1^2 \left(coth\ k_1 h \cdot coth\ k_2 h - \frac{7}{2}\right)\right\} \cos(S_1 + S_2) \\ &+ \frac{1}{g}\left\{-\sigma_1 B_{24} coth(k_1 - k_2) h - \frac{1}{2} a_1 a_2 \sigma_1^2 (2coth\ k_1 h \cdot coth\ k_2 h - 3)\right\} \cos(S_1 - S_2). \end{aligned}\right\} \quad (10)$$

The terms on the right-hand side of this equation correspond in sequence to the wave components A_{01}, A_{12}, A_{02}, A_{24}, A_{13} and A_{11}. Against what we had expected initially, our preliminary experimental measurements of the wave profile at $Ur = 42$ indicate that the agreement with the predictions based on Eq. (10) is unsatisfactory. The presence of the spectral component A_{03} is evident in experiments and the measured celerities of A_{01} and A_{12} are not consistent with the dispersion relation of linear wave theory. This discrepancy can be also detected from the numerical results shown in Figs. 2 and 3. To improve the agreement, we conveniently make use of the numerical results; the amplitudes and coefficients introduced in Eqs. (8) and (10) are determined from

$$\left.\begin{aligned} a_1 &= \frac{H}{2}\xi_{01} \\ a_2 &= \frac{H}{2}\xi_{12} \\ B_{21} &= \frac{H}{2}\,\frac{4\xi_{02} g - \frac{H}{2}\xi_{01}^2 \sigma_1^2 (3 - coth^2 k_1 h)}{8\sigma_1 coth\ 2k_1 h} \\ B_{22} &= \frac{H}{2}\,\frac{\xi_{24} g - \frac{H}{2}\xi_{12}^2 \sigma_1^2 (3 - coth^2 k_2 h)}{4\sigma_1 coth\ 2k_2 h} \\ B_{23} &= \frac{H}{2}\,\frac{2\xi_{13} g - \frac{H}{2}\xi_{01}\xi_{12}\sigma_1^2 (7 - 2coth\ k_1 h\ coth\ k_2 h)}{6\sigma_1 coth(k_1 + k_2) h} \\ B_{24} &= \frac{H}{2}\,\frac{2\xi_{13} g - \frac{H}{2}\xi_{01}\xi_{12}\sigma_1^2 (3 - 2coth\ k_1 h\ coth\ k_2 h)}{2\sigma_1 coth(k_1 - k_2) h} \end{aligned}\right\} \quad (11)$$

and the dispersion relations from Eq. (5). Furthermore, we add the potential function of A_{03} that results from the third-order interactions to Ep. (8). Then the velocity potential in the absence of any other components is given by

$$\phi' = \phi + B_{31}\frac{cosh\ 3k_1 (h+z)}{sinh\ 3k_1 h} sin\ 3S_1 \quad (12)$$

where

$$B_{31} = \frac{a_1 \sigma_1^2 k_1 \left\{B_{21}(2coth\ k_1 h \cdot coth\ 2k_1 h - 3) + \frac{1}{2}\xi_{02}(1 - tanh^2 k_1 h)\right\}}{3\sigma_1^2\ coth\ 3k_1 h - g k_1} \quad (13)$$

An additional term associated with the fundamental component is obtained, but excluded from this equation because its contribution to the behavior of the velocity field is extremely small. The corresponding wave profile is now given by

$$\left.\begin{aligned} \eta'(x,\ t) &= \eta(x,\ t) + \frac{1}{g}\left\{B_{21} a_1 \sigma_1 k_1 (3 - coth\ k_1 h \cdot coth\ 2k_1 h) + \frac{1}{2} a_1 \sigma_1^2 \xi_{02}\right. \\ &\left. + \frac{1}{8} a_1^3 \sigma_1^2 k_1 coth\ k_1 h\right\} \cos 3S_1 \end{aligned}\right\} \quad (14)$$

The dispersion relation for primary and secondary free waves is now given as that of Stokes third-order wave theory.

An exression for the mass-transport velocity may be obtained by representing the Lagrangian velocity of a given particle at the instantaneous

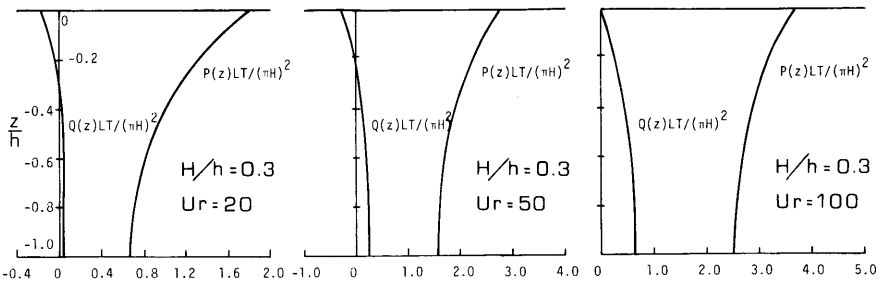

Fig. 4 : Distributions of the steady component $P(z)LT/(\pi H)^2$ and the spatially varying component $Q(z)LT/(\pi H)^2$ of the mass transport.

position (ξ, ζ) as a Taylor series of the Eulerian horizontal velocity at a fixed position $(0, 0)$:

$$u(\xi, \zeta, t) = u(0, 0, t) + \xi \frac{\partial u}{\partial x}(0, 0, t) + \zeta \frac{\partial u}{\partial z} + \frac{\xi^2}{2} \frac{\partial^2 u}{\partial x^2} + \xi\zeta \frac{\partial^2 u}{\partial x \partial z} + \frac{\zeta^2}{2} \frac{\partial^2 u}{\partial z^2} + \cdots\cdots \quad (15)$$

where

$$\xi = \int u(0, 0, t')\, dt', \quad \zeta = \int w(0, 0, t')\, dt'$$

If u, w, ξ and ζ are now expanded as power series in wave steepness,

$$\left.\begin{aligned} u &= u_1 + u_2 + u_3 + \cdots \\ w &= w_1 + w_2 + w_3 + \cdots \\ \xi &= \xi_1 + \xi_2 + \xi_3 + \cdots \\ \zeta &= \zeta_1 + \zeta_2 + \zeta_3 + \cdots \end{aligned}\right\} \quad (16)$$

we obtain the mass-transport velocity extended to the third-order approximation in the form

$$\left.\begin{aligned} U_M = \Bigg(& \overline{\xi_1 \frac{\partial u_1}{\partial x}} + \overline{\zeta_1 \frac{\partial u_1}{\partial z}} \Big) + \Big(\overline{\xi_2 \frac{\partial u_1}{\partial x}} + \overline{\xi_1 \frac{\partial u_2}{\partial x}} \\ & + \overline{\frac{\xi_1^2}{2} \frac{\partial^2 u_1}{\partial x^2}} + \overline{\zeta_2 \frac{\partial u_1}{\partial z}} + \overline{\zeta_1 \frac{\partial u_2}{\partial z}} + \overline{\frac{\zeta_1^2}{2} \frac{\partial^2 u_1}{\partial z^2}} \\ & + \overline{\xi_1 \zeta_1 \frac{\partial^2 u_1}{\partial x \partial z}} \Bigg) \end{aligned}\right\} \quad (17)$$

where an overbar denotes a temporal mean and the Euler velocity periodic in time vanishes in taking the time average. Substituting Eq. (12) into Eq. (17) yields

$$U_M = P(z) + Q(z)\cos\Delta k \cdot x \quad (18)$$

where

$$P(z) = \frac{a_1^2 \sigma_1 k_1 \cosh 2k_1(h+z)}{2\sinh^2 k_1 h} + \frac{a_2^2 \sigma_1 k_2 \cosh 2k_2(h+z)}{\sinh^2 k_2 h}$$

$$Q(z) = -\left\{ \frac{a_1 B_{24} k_2 (k_1 - k_2) \cosh k_2(h+z)}{2\sinh k_1 h \sinh (k_1 - k_2) h} + \frac{a_2 B_{21} k_1 (2k_1 + k_2) \cosh (2k_1 + k_2)(h+z)}{\sinh 2k_1 h \sinh k_2 h} \right\} + \frac{1}{4} a_1^2 a_2 \sigma_1 \left\{ \frac{k_1^2 \cosh k_2(h+z)}{\sinh^2 k_1 h \cdot \sinh k_2 h} - \frac{k_2^2 \cosh (2k_1 + k_2)(h+z)}{\sinh^2 k_1 h \cdot \sinh k_2 h} \right\}$$

The second-order quantity $P(z)$ assumes uniform flow in the x direction while the third-order quantity $Q(z)$ varies spatially according to $\cos\Delta kx$. Note here that $\cos\Delta kx = 1$ at $x = m\ Lov$ and $\cos\Delta kx = -1$ at $x = (m+1/2)\ Lov$, with m being an arbitrary integer. If no nonlinear interaction occurs, omitting a_2 in Eq. (18) eventually reduces to the well-known formula of Stokes' drift.

Fig. 4 shows the distributions of $P(z)$ and $Q(z)$ expressed in a dimensionless form at $Ur = 20$, 50 and 100. It should be remarked that the spatially varying component $Q(z)$ becomes more pronounced as Ur increases.

The predicted mass transport is unsteady by virtue of the $\cos\Delta kx$ terms in Eq. (18). This might give rise to a circulating flow in a closed-ended wave channel. We require the total horizontal transport to be zero and further assume the steady mass-transport velocity $P(z)$ to vanish everywhere along the wave channel. This rather crucial assumption is made since our preliminary experiments indicate that the mass-transport velocity vanishes identically at $x = (m \pm 1/4) Lov$, i.e., when $\cos\Delta kx = 0$. For a return flow in accordance with the unsteady dnift $Q(z)\cos\Delta kx$, we assume two types of parabolic distribution as

$$U_{M1} = Q(z)\cos\Delta kx - C_1(-h+z)(h+z) \times \cos\Delta kx \quad (19)$$

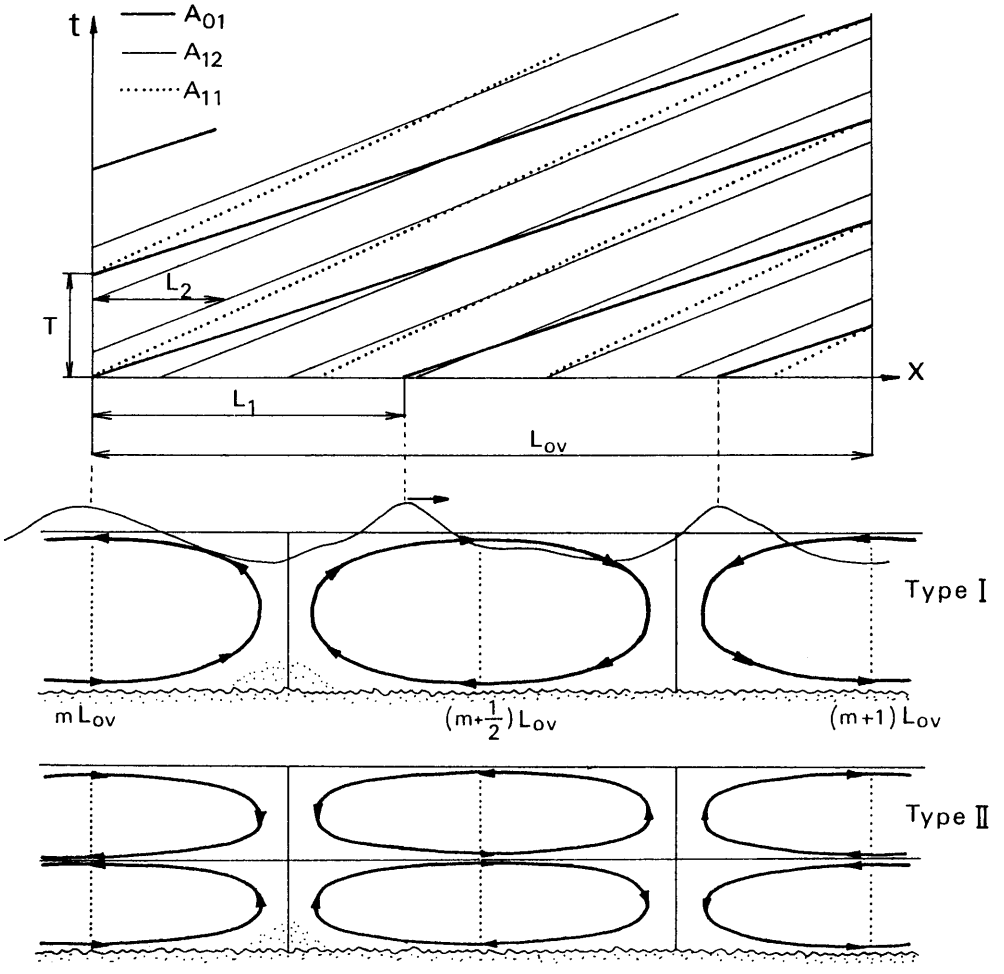

Fig. 5 : Circularion patterns and $x-t$ diagram of the spectral components.

and

$$U_{M11}=Q(z)\cos\Delta kx-C_{11}z\,(h+z)\cos\Delta kx \tag{20}$$

Requiring the total horizontal flow due to the mass transport to be zero, arbitrary constants C_1 and C_{11} are given as

$$C_I=\frac{3}{4h^3}\left\{\frac{a_1B_{24}(k_1-k_2)\sinh k_2h}{\sinh k_1h\,\sinh(k_1-k_2)h}+\frac{2a_2B_{21}k_1\sinh(2k_1+k_2)h}{\sinh 2k_1h\,\sinh k_2h}\right\}$$
$$-\frac{3}{8h^3}\left\{\frac{a_1^2a_2\sigma_1k_1^2}{k_2\sinh^2k_1h}-\frac{a_1^2a_2\sigma_1k_2^2\sinh(2k_1+k_2)h}{(2k_1+k_2)\sinh^2k_1h\,\sinh k_2h}\right\} \tag{21}$$

$$C_{II}=4C_I \tag{22}$$

COMPARISON WITH EXPERIMENT

A wave channel used in the experiments is 26m long, 0.6m wide, 1.0m deep and glazed on one side. Waves were generated by a wave-paddle, sinusoidally oscillating in a horizontal plane with different strokes at the bottom and still water levels. At the end of the channel a gravel beach of slope 1/10 was constructed as a wave absorber. Over the full length of the channel the bottom was covered with a 10cm thick horizontal sand bed with a mean particle diameter of 290μm. For measurements of the mass-transport velocity, potassium permangnate grains glued to a pole were inserted over the water depth at a particular point. The movement of the center of a cloud of dye was then read at every 10sec. The temporal wave profiles were measured using a capacitance type wave gauge. To ensure a steady state all

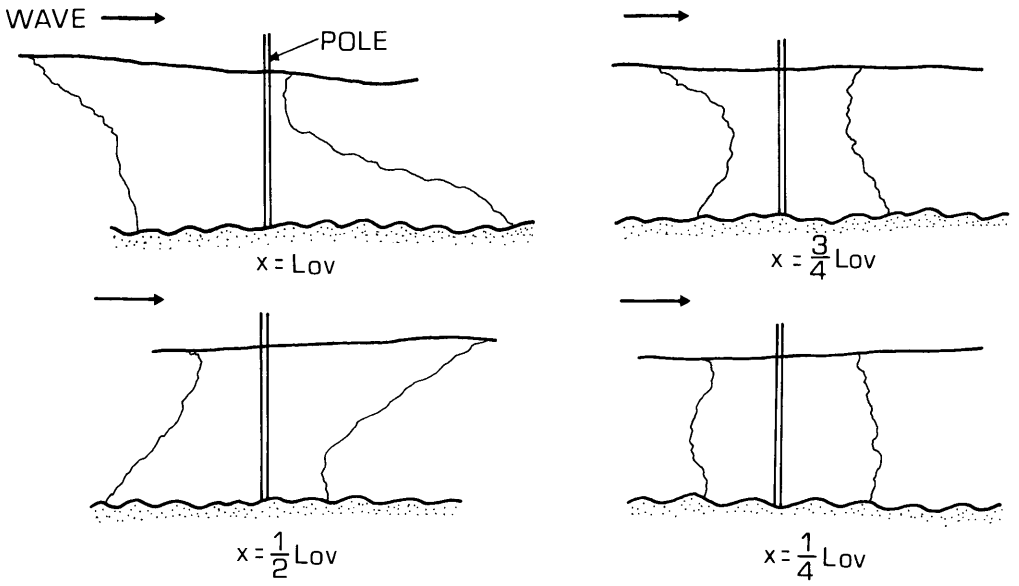

Fig. 6 : Profiles of the cloud of dye at various positions for $Ur=111$. The profiles were traced from photos taken 10sec. after inserting the dye.

measurements were done after ripples of the equilibrium form being developed and were terminated before the large scale undulation of the sand bed being developed.

Experiments were conducted with a constant depth of 20cm and wave periods of 1.2, 1.7, 2.0 and 2.4sec. The wave height H varied between 6cm and 9cm. The Ursell number $Ur=HL^2/h^3$ thus ranged from 30 to 111. Measurements were related to the overtake length Lov, a location of which was computed from

$$L_{ov}=\frac{1}{2}\frac{C_1C_2}{C_1-C_2}T \qquad (23)$$

where celerities c_1 and c_2 for a given Ur were determined from Fig. 3. The distance of Lov was then adjusted by examing the measured wave profile.

The observed drift of dye, an example of which is presented in Fig. 6, indicates the occurence of circulating currents. Fig. 7 (a)-Fig. 7 (d) show the comparison between the measured and predicted mass-transport velocities over the depth for $Ur=50$ and $Ur=111$. The behavior of the mass transport profiles is rather well predicted by Eq. (19) (i.e., type I) including the data not shown here.

In Fig. 8 (a)-Fig. 8 (d) the measured wave profiles are compared with the porfiles computed from Eq. (14) at Lov and $Lov/2$. Slight discrepancy observed at $Ur=111$ may be due to the presence of higher order components that are not included in Eq. (14).

CONCLUSIONS

The solution of the mass transport in unsteady shallow-water waves has been derived semi-analytically using the numerical results obtained previously by one of the present writers. The resulting exression for the mass-transport velocity consists of the steady and spatially varying components. The unsteady part of the drift increases its strength with the increasing Ursell number. This behavior of the mass transport induces the circulating currents in the closed-ended wave channel. The results of experiments compare favorably with the theoretical predictions.

The results obtained in this study may be of significant interest in the explanation of the formation of multiple offshore bars, particularly if the grain of the bed material is fine and if the effect of superposed tidal currents is less significant.

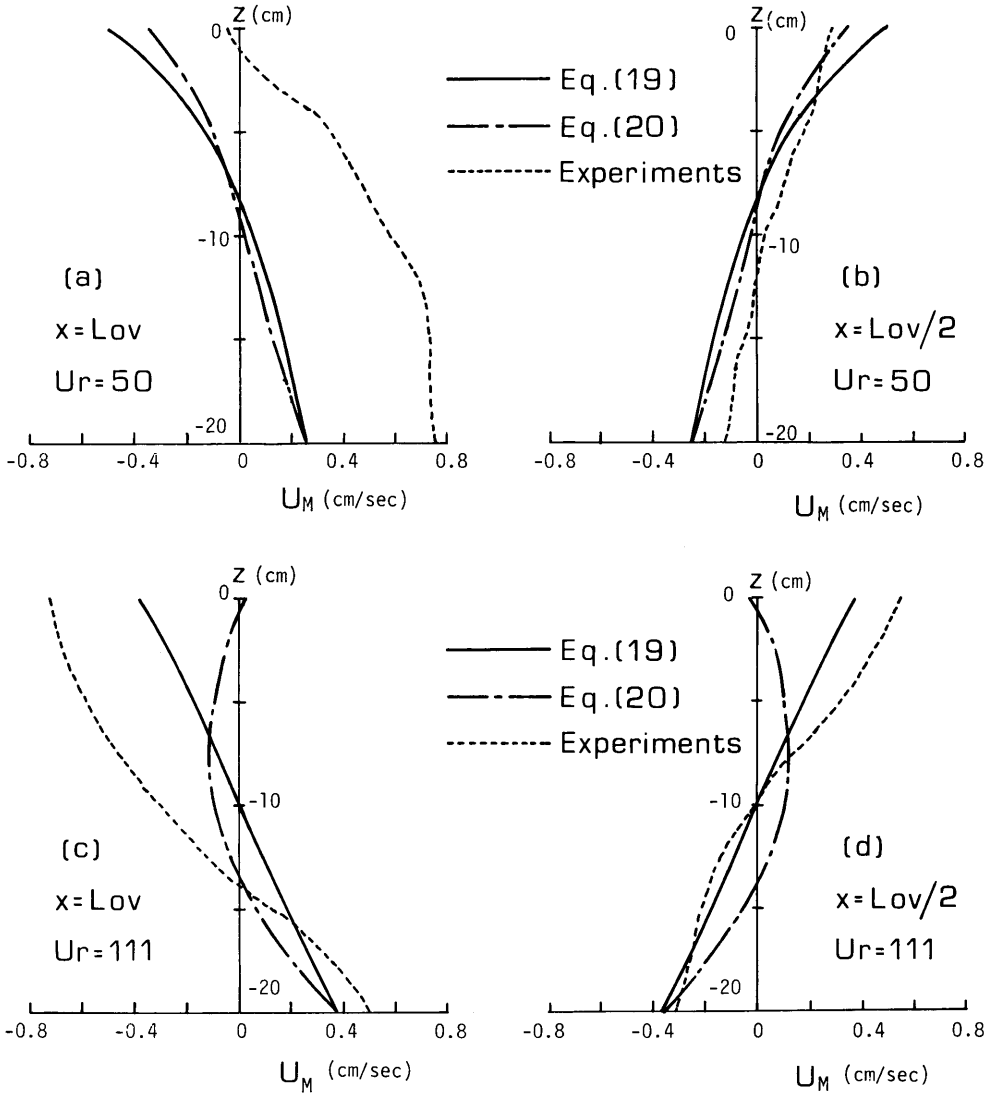

Fig. 7 : Distributions of the mass transport over the depth.

REFERENCES

Fontanet, P., Thâorie de la generatin de la houle cylindrique par un batteur plan, La Houille Blanche, 3-61 *(1)*, 174-197 (2), 1961.

Hamada, T., The secondary interactions of surface waves, Rep. Port and Harbour Tech. Res. Inst., *10*, 1-28, 1969.

Isaacson, M. de St. Q., The second approximation to mass transport in croidal waves, *J. Fluid Mech.*, *78*, 445-457, 1976.

Ishida, A., J. Hirosawa and Y. Nishigaki, Double Fourier components of deforming shallow water waves simulated with KdV equations, Proc. 26th Japanese Conference on Coastal Eng., 16-20, 1979.

Ishida, A., H. Takahashi and K. Kanazawa, Deformation of shallow water waves on a constant depth, Proc. 27th Japanese Conference on Coastal Eng., 20-24, 1980.

Ishida, A. and H. Takahashi, Numerical analysis of shallow-water wave deformation in a constant depth region, *Coastal Eng. in Japan*, *24*, 1-18,

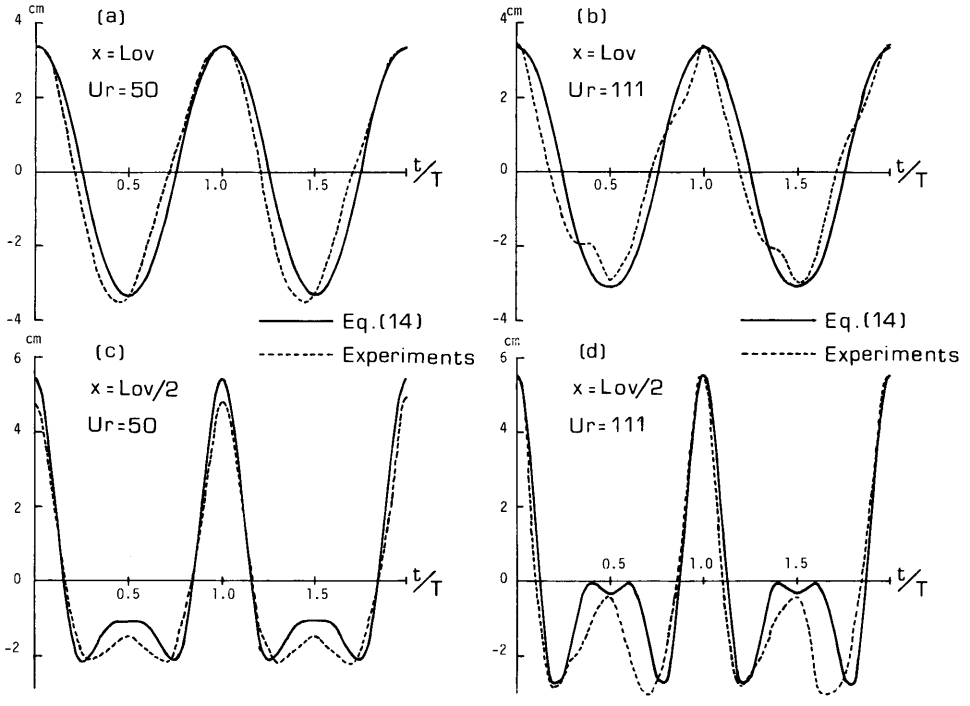

Fig. 8 : Comparison of the measured and computed wave profiles.

1981.

Ishida, A., W. Kioka and K. Asada, Mass transport velocity of nonlinear shallow water waves, *J. Japan Soc. Fluid Mech., 2,* 371-380-1983.

Longuet-Higgins, M. S., Mass transport in water waves, *Phil. Trans. Roy. Soc. London, A903,* 535-581, 1953.

Mei, C. C., *The applied dynamics of ocean surface waves,* 740pp., John Wiley&Sons, New York, 1983.

Phillips, O. M., On the dynamics of unsteady gravity waves of finite amplitude-Partl. The elementary interactions, *J. Fluid Mech., 9,* 193-217, 1960.

Sleath, J. F. A., A second approximation to mass transport by water waves, *J. Marine Res., 30,* 295-304, 1972.

Stokes, G. G., On the theory of oscillatory waves, Proc. Cambridge Phil. Soc., *8,* 441-455, 1847.

Ünlüata, U. and C. C. Mei, Mass transport in water waves, *J. Geophy. Res., 75,* 7611-7618, 1970.